Forkhead Transcription Factor FoxO1 in Adipose Tissue Regulates Energy Storage and Expenditure

Jun Nakae,[1] Yongheng Cao,[1] Miyo Oki,[1] Yasuko Orba,[2] Hirofumi Sawa,[3] Hiroshi Kiyonari,[4] Kristy Iskandar,[5] Koji Suga,[1] Marc Lombes,[6] and Yoshitake Hayashi[5]

OBJECTIVE—Adipose tissue serves as an integrator of various physiological pathways, energy balance, and glucose homeostasis. Forkhead box–containing protein O subfamily (FoxO) 1 mediates insulin action at the transcriptional level. However, physiological roles of FoxO1 in adipose tissue remain unclear.

RESEARCH DESIGN AND METHODS—In the present study, we generated adipose tissue–specific FoxO1 transgenic mice (adipocyte protein 2 [aP_2]-FLAG-Δ256) using an aP_2 promoter/enhancer and a mutant FoxO1 (FLAGΔ256) in which the carboxyl terminal transactivation domain was deleted. Using these mice, we analyzed the effects of the overexpression of FLAGΔ256 on glucose metabolism and energy homeostasis.

RESULTS—The *aP_2-FLAG-Δ256* mice showed improved glucose tolerance and insulin sensitivity accompanied with smaller-sized adipocytes and increased adiponectin (adipoq) and Glut 4 (Slc2a4) and decreased tumor necrosis factor α (Tnf) and chemokine (C-C motif) receptor 2 *(Ccr2)* gene expression levels in white adipose tissue (WAT) under a high-fat diet. Furthermore, the *aP_2-FLAG-Δ256* mice had increased oxygen consumption accompanied with increased expression of peroxisome proliferator–activated receptor γ coactivator (PGC)-1α protein and uncoupling protein (UCP)-1 *(Ucp1)*, *UCP-2* (Ucp2), and β3-AR *(Adrb3)* in brown adipose tissue (BAT). Overexpression of FLAGΔ256 in T37i cells, which are derived from the hibernoma of SV40 large T antigen transgenic mice, increased expression of PGC-1α protein and Ucp1. Furthermore, knockdown of endogenous FoxO1 in T37i cells increased Pgc1α *(Ppargc1a)*, Pgc1β *(Ppargc1b)*, Ucp1, and Adrb3 gene expression.

CONCLUSIONS—These data suggest that FoxO1 modulates energy homeostasis in WAT and BAT through regulation of adipocyte size and adipose tissue–specific gene expression in response to excessive calorie intake. ***Diabetes*** **57:563–576, 2008**

The incidence of obesity has been increasing worldwide. Obesity is the result of energy imbalance, and it can develop when energy intake exceeds energy expenditure (1). Energy intake is almost entirely determined by food intake (minus whatever fails to be absorbed), which is regulated by leptin, insulin, adiponectin, interleukins, cholecystokinin, peptide-$YY_{3–36}$, ghrelin, glucagon-like peptide-1, malonyl CoA, and long-chain fatty acids through actions on the mediobasal hypothalamus or the nucleus of the solitary tract in the brainstem (2–5). On the other hand, energy expenditure has more components, including basal metabolism, physical activity, and adaptive thermogenesis (1).

In situations of excess energy intake, excess calories will be stored primarily in adipose tissue. However, in a situation of chronic calorie overload, subcutaneous adipose tissue eventually reaches its upper limit for further triglyceride storage, and this may trigger adipose inflammation as well as lipid "spillover." This means that energy storage will be partitioned toward the visceral fat depot and subsequently into ectopic fat depots, which include intrahepatocellular and intramyocellular lipids, both of which will have direct negative effects on insulin action in these tissues (1,6). The capacity of fat storage could be determined by genetic programming of recruitment of new adipocytes or by neuroendocrine interactions as well as adipose tissue inflammation. It has been suggested that an increased adipocyte size is associated with insulin resistance (7). Therefore, the prevention of the generation of enlarged adipocytes might lead to inhibition of development of insulin resistance in the whole body.

Adaptive thermogenesis is defined as heat production in response to cold exposure or overfeeding and it serves the purpose of protecting the organism from cold exposure or regulating energy balance after changes in diet. Diet is a potent regulator of adaptive thermogenesis. Starvation or calorie restriction decreases resting metabolic rate. In contrast, feeding increases energy expenditure. Brown adipose tissue (BAT) and skeletal muscle are the two major organs involved in adaptive thermogenesis (8). While rodents have prominent brown fat depots, this is not the case in larger mammals, including humans, although there may be brown fat cells dispersed among the adipocytes of white adipose tissue (WAT) (1). The adaptive thermogenic program in both BAT and skeletal muscle involves the stimulation of mitochondria biogenesis, increased fatty acid oxidation, and the uncoupling of oxida-

From the [1]21st Century Center of Excellence (COE) Program for Signal Transduction Disease: Diabetes Mellitus as Model, Department of Clinical Molecular Medicine, Division of Diabetes, Digestive and Kidney Disease, Kobe University Graduate School of Medicine, Kobe, Japan; the [2]Laboratory of Molecular and Cellular Pathology, Hokkaido University Graduate School of Medicine, Sapporo, Japan; the [3]21st Century COE Program for Zoonosis Control, Department of Molecular Pathobiology, Research Center for Zoonosis Control, Hokkaido University, Sapporo, Japan; the [4]Laboratory for Animal Resources and Genetics Engineering Team, RIKEN Center for Developmental Biology, Hyogo, Japan; the [5]Division of Molecular Medicine and Medical Genetics, International Center for Medical Research and Treatment, Kobe University Graduate School of Medicine, Kobe, Japan; and the [6]Institut National de la Santé et de la Recherch Médicale, Faculte de Medecine, Paris, France.

Address correspondence and reprint requests to Jun Nakae, MD, Department of Clinical Molecular Medicine, Division of Diabetes, Digestive and Kidney Diseases, Kobe University Graduate School of Medicine, 7-5-1 Kusunoki-cho, Chuo-ku, Kobe 650-0017, Japan. E-mail: nakaej@med.kobe-u.ac.jp.

Received for publication 26 May 2007 and accepted in revised form 12 December 2007.

Published ahead of print at http://diabetes.diabetesjournals.org on 27 December 2007. DOI: 10.2337/db07-0698.

Additional information for this article can be found in an online appendix at http://dx.doi.org/10.2337/db07-0698.

aP_2, adipocyte protein 2; BAT, brown adipose tissue; CN, constitutively nuclear; FoxO, forkhead box–containing protein O subfamily; PGC, PPAR γ coactivator; PPAR, peroxisome proliferators–activated receptor; shRNA, short-hairpin RNA; UCP, uncoupling protein; WAT, white adipose tissue.

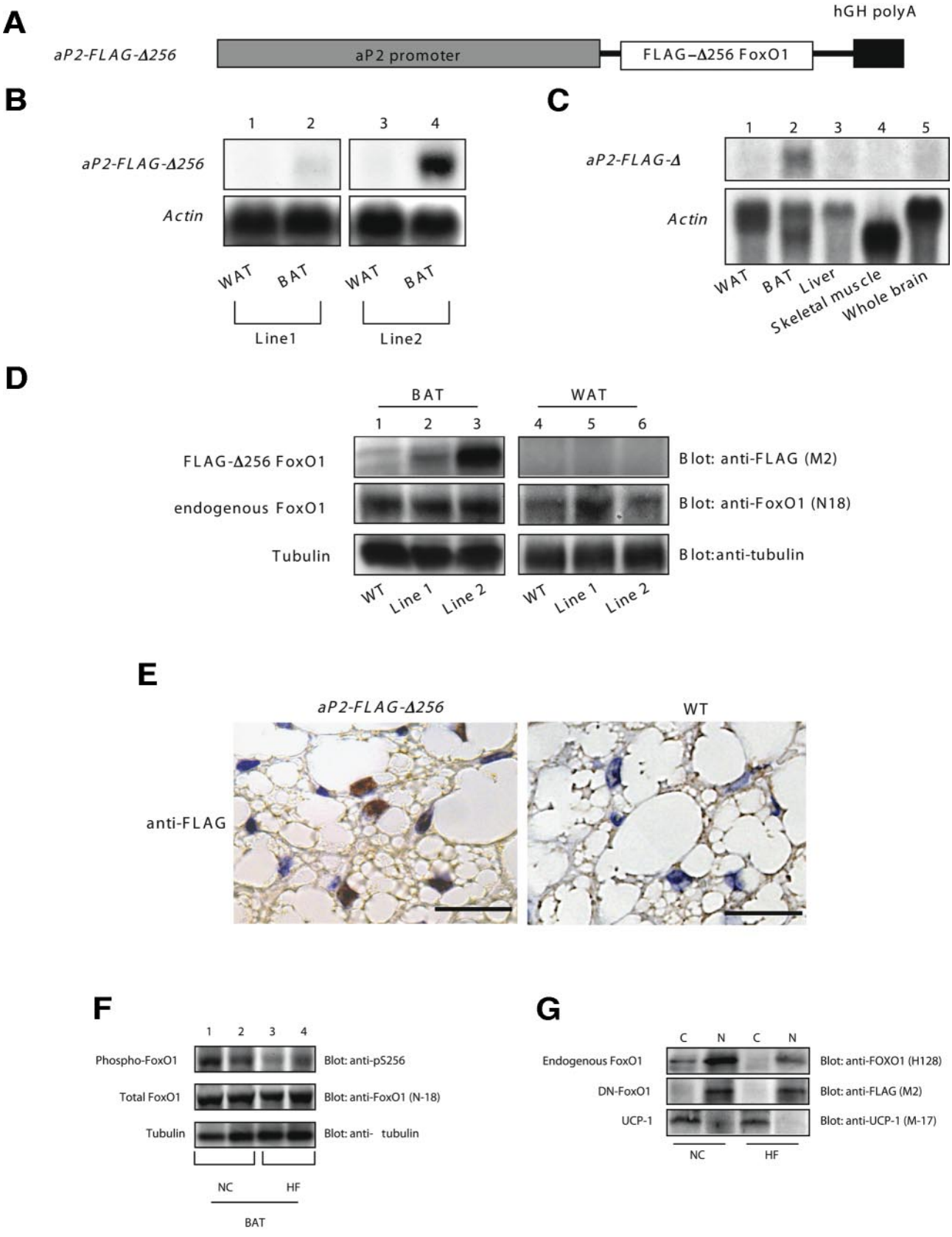

FIG. 1. Generation of transgenic mice expressing a mutant FoxO1 driven by the *aP2* promoter. *A*: Diagram of the transgenic construct. In addition to 5.4 kb of the *aP2* promoter, the construct contains the *FLAG-Δ256 FoxO1* cDNA and the human GH polyadenylation sequences. *B*: Northern blotting of transgene expression in WAT (*lanes 1* and *3*) and BAT (*lanes 2* and *4*) from line 1 (*lanes 1* and *2*) and line 2 (*lanes 3* and *4*). *C*: Tissue survey of transgene expression in line 2 at the age of 6 months under a normal diet. Total RNA was isolated from the tissues indicated at the bottom of the autoradiogram and analyzed by Northern blotting using a *FoxO1* cDNA probe. *D*: Western blotting of transgene expression in BAT (*lanes 1-3*) and WAT (*lanes 4–6*) from wild-type (*lanes 1* and *4*), line 1 (*lanes 2* and *5*), and line 2 (*lanes 3* and *6*) transgenic male mice at the age of 6 months under a normal diet. The *top panel* shows immunoblotting of tissue lysates (50 μg) with anti-FLAG mouse monoclonal antibody

tive phosphorylation (9). In response to cold exposure, peroxisome proliferators–activated receptor (PPAR) γ coactivator (PGC)-1α expression is increased. PGC-1α enhances the expression of BAT-specific uncoupling protein (UCP)-1, which dissipates the proton gradient across the inner mitochondrial membranes that is produced by the action of the electron transport chain (9,10). The essential role of PGC-1α in adaptive thermogenesis is demonstrated by the observation that PGC-1α knockout mice are unable to withstand a cold stress with reduced UCP-1 expression (11).

Insulin and/or IGF-1 signaling are also involved in the development and functional maintenance of BAT. BAT-specific insulin receptor knockout mice (BATIRKO) showed an age-dependent atrophy of BAT (12). Cells lacking both insulin receptor substrate-1 and -3 failed to differentiate with reduced expression of *Ppargc1a* and *Ucp1* (13). These effects of insulin/IGF-1 and insulin receptor substrates on the function of brown adipocytes might be mediated through phosphatidylinositol 3-kinase and Akt (14). However, currently there is very little known about downstream targets of phosphatidylinositol 3-kinase and Akt and transcriptional regulation by insulin/IGF-1.

Forkhead transcription factors of the forkhead box–containing protein O subfamily (FoxO) are phosphorylated mainly by Akt and regulated by insulin/IGF-1. The FoxO family is conserved across many species (15). In mammals, InsR/IGF1R–phosphatidylinositol 3-kinase–Akt signaling inhibits transcription by FoxO1, FoxO3a, and FoxO4. These proteins possess a forkhead DNA binding domain consisting of ~110 amino acids and a transactivation domain in the C terminus. FoxOs bind to consensus FoxO binding sites [T(G/A)TTTT(G/T)] in the promoter region of their target genes and activate gene expression (16). It has been reported that *FoxO*s were expressed in adipose tissue and that a constitutively nuclear mutant FoxO1 inhibited differentiation of the preadipocyte cell line 3T3-F442A cells and that haploinsufficiency of *FoxO1* reduced cell size and increased cell numbers of white adipocytes of mice under a high-fat diet (17). However, there have been no reports about physiological roles of FoxO1 in adipose tissue, which include both WAT and BAT using a tissue-specific manner.

In the present study, we generated adipose tissue–specific *FoxO1* transgenic mice of a mutant FoxO1 (FLAGΔ256) (18) under the control of the mouse adipocyte protein 2 (aP_2) promoter. Using transgenic mice, we demonstrated that overexpression of the FLAGΔ256 in adipose tissue ameliorated insulin resistance induced by a high-fat diet accompanied with smaller sizes of adipocytes in WAT and increased oxygen consumption through increased expression of PGC-1α protein. These data indicate that FoxO1 in adipose tissues might regulate energy homeostasis through regulation of adipose tissue–specific gene expression.

RESEARCH DESIGN AND METHODS

Antibodies. We purchased anti-FLAG (M2), anti-tubulin, and anti–UCP-1 (M-17) from Sigma; anti-FOXO1 (N18 and H128) and anti–PGC-1 (H-300) from Santa Cruz Biotechnology; anti-HA monoclonal antibody (12CA5) from Roche; and anti–phospho-FOXO1 (pS256 and pT24) and anti–4E-BP1 from Cell Signaling Technology. We used anti-FOXO1 antibody (H128) only when we tried to discriminate endogenous FoxO1 from FLAGΔ256, clearly because the epitope of H128 was the carboxyl terminus of FOXO1, which FLAG-Δ256 did not have.

Generation of adipose tissue–specific FoxO1 transgenic mice. We cloned a mutant FoxO1 cDNA, bearing a truncated FoxO1 (a.a 1-255) (Δ256) that has no transactivation domain and a FLAG peptide tag, into the *Sma*I site of plasmid pCMV5-aP2, in which the *Cla*I and *Sma*I-treated 5.4-kb promoter/enhancer fragment of the mouse *aP2* gene was subcloned into the *Cla*I/*Sma*I-treated pCMV5/cMyc vector (19). We excised the transgene with *Cla*I and *Xho*I and gel-purified and injected it into fertilized eggs of FVB × Bl6 hybrid mice. The resulting embryos were implanted into CD-1 foster mothers. We screened offspring for transgene transmission by PCR. Of five independent transgenic lines obtained, two founders transmitted the transgene through the germline. Primers for genotypying were FLAG-S1: 5′-atggactacaaagacgatgac-3′ and SE1AS: 5′-gtcgagttggactggttaaac-3′.

Animal studies, analytical procedures, glucose tolerance, and insulin tolerance tests. We used only male mice for the following analyses. Animals were fed a standard diet and water ad libitum in sterile cages in a barrier animal facility with 12-h/12-h light/dark cycle. All experimental protocols using mice were approved by the animal ethics committee of Kobe University Graduate School of Medicine. A high-fat diet was begun at weaning (4 weeks of age) and continued for 15 weeks. We used the same high-fat diet as described previously (20). We measured glucose levels with a Glutest Pro (Sanwa Kagaku Kenkyusho) and insulin, leptin, and resistin by radioimmunoassay (Linco). We carried out all assays in duplicate. Each value represents the means of two independent determinations. Analysis was limited to male mice, as they are more susceptible to insulin resistance and diabetes. Glucose tolerance and insulin tolerance test were performed as described (21). Hepatic glycogen measurement was performed as described previously (21). Computed tomography was performed using a LaTheta LCT-100M (Aloka).

Measurement of oxygen consumption. Six-month-old mice under the normal diet and mice under the high-fat diet for 15 weeks were monitored individually in a metabolic cage (O_2/CO_2 metabolism measuring system for small animals model MK-5000; Muromachi Kikai) with free access to a normal diet and drinking water for 48 h. Each cage was monitored for oxygen consumption at 5-min intervals throughout the 48-h period. Total oxygen consumption was calculated as accumulated oxygen uptake for each mouse divided by its body weight. We performed oxygen consumption of three to four mice in each genotype in each condition (normal-diet or high-fat–dieted condition). Representative graphs were drawn from the mean and SE calculated from data obtained in each measurement.

RNA isolation, real-time PCR, and Northern blotting. Isolation of total RNA from tissues and cells was performed using an SV Total RNA Isolation System (Promega) according to manufacturer's protocol. Real-time PCR was also performed as described previously (17). The primers used in this study were described in the online appendix Table 1 (available at http://dx.doi.org/10.2337/db07-0698). Northern blotting was performed according to the standard techniques. For preparation of the probe for *FoxO1*, we treated pFLAG CMV-2 WT FoxO1 (22) with *Eco*RI, and the probe β-actin used here was described previously (18).

Western blotting. We homogenized tissues in buffer containing 50 mmol/l Tris/HCl (pH 8.0), 250 mmol/l NaCl, 1% NP40, 0.5% deoxycholate, 0.1% SDS, and protease inhibitors (Roche Diagnostics). After centrifugation to remove insoluble material, each 50 μg of lysate was electrophoresed in 8% or 14% SDS-PAGE, and Western blotting was performed using indicated antibodies.

Immunohistochemistry and histological analysis. For immunohistochemistry of WAT and BAT, we incubated WAT and BAT overnight in 4% paraformaldehyde and embedded them in paraffin. We then mounted consecutive 5-μm sections on slides. After rehydration and permeabilization, we

(M2) (SIGMA). The *middle panel* shows immunoblotting with anti-FOXO1 (N18) antibody. The *bottom panel* shows immunoblotting with anti-tubulin mouse monoclonal antibody (Sigma). *E*: Immunohistochemistry of BAT from transgenic (*left panel*) and wild-type (*right panel*) mice using OctA-Probe (D-8) (sc-807; Santa Cruz Biotechnology). Scale bars indicate 20 μm. *F*: Western blotting of phosphorylated FoxO1 in BAT from wild-type mice under a normal diet (*lanes 1* and *2*) at the age of 6 months or under a 15-week high-fat diet (*lanes 3* and *4*) in the fed state. The *top panel* shows Western blotting with anti–phospho-FOXO1 (pS256), the *middle panel* shows Western blotting with anti-FOXO1 (N18), and the *bottom panel* shows Western blotting with anti-tubulin antibody. *G*: Fractionation of cytoplasmic (C) and nuclear(N) extracts of BAT from transgenic mice under a normal diet at the age of 6 months and a 15-week high-fat diet in the fed state. The *top panel* shows Western blotting of endogenous FoxO1 with anti-FOXO1 (H128), the *middle panel* shows Western blotting of DN FoxO1 with anti-FLAG (M2), and the *bottom panel* shows Western blotting of UCP-1 using anti–UCP-1 (M17).

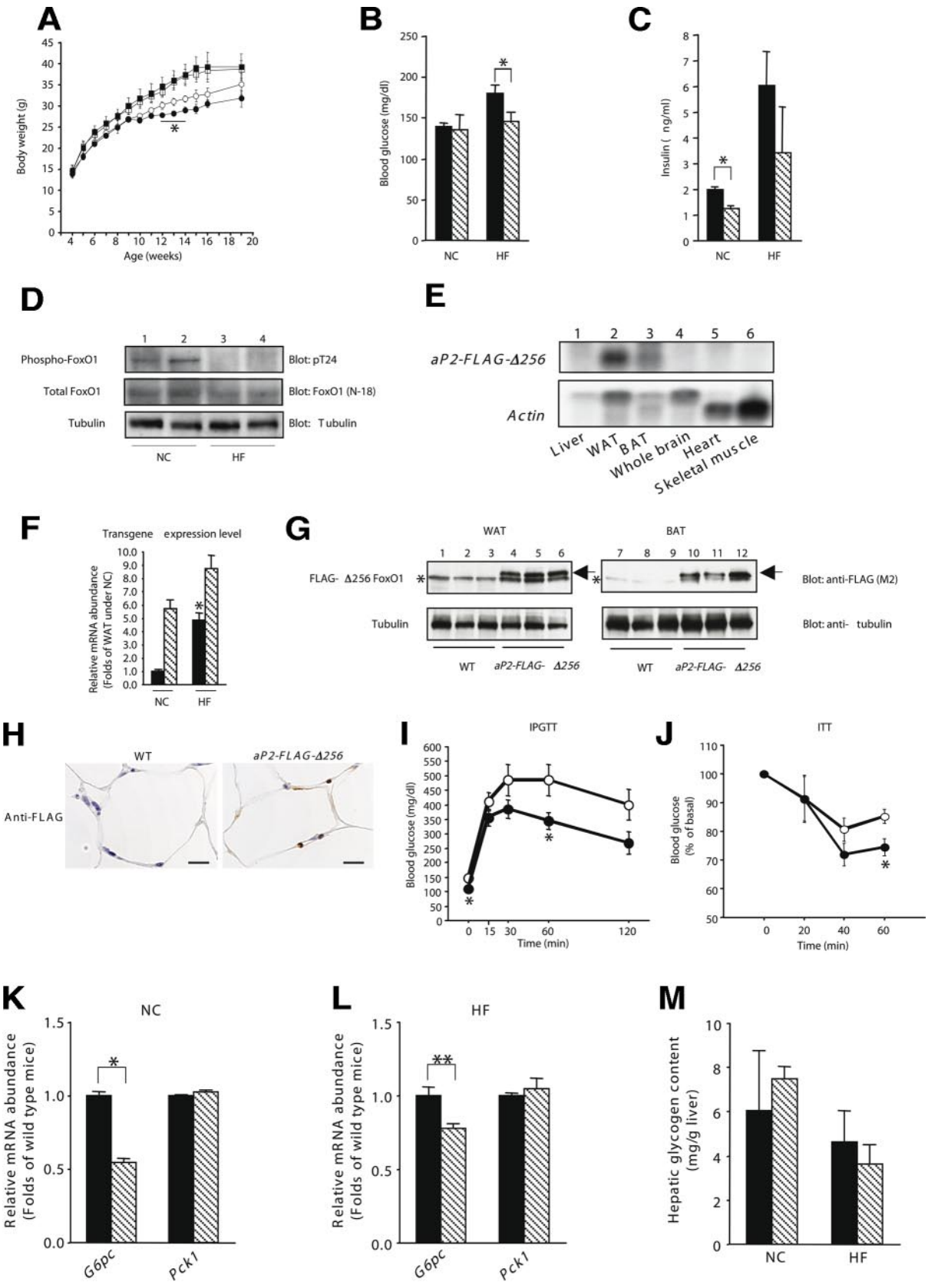

FIG. 2. Metabolic characterization of *FoxO1* transgenic mice. *A*: Body weight of wild-type and transgenic mice under the normal and high-fat diets. Data represent means ± SE of 20 male mice for each genotype. ○, wild-type under a normal diet; ●, transgenic mice under a normal diet; □, wild-type mice under a high-fat diet; ■, transgenic mice under a high-fat diet. An asterisk indicates a statistically significant difference between wild-type and transgenic mice under a normal diet from the age of 12 to 14 weeks ($P < 0.05$ by one-factor ANOVA). *B*: Fed blood glucose levels of wild-type (■) and transgenic (▨) mice under normal chow at the age of 6 months (NC) and a 15-week high-fat diet (HF). Data represent means ± SE of 20 male mice for each genotype. *Statistically significant difference between wild-type and transgenic mice under high-fat diet conditions ($P < 0.05$ by one-factor ANOVA). *C*: Fed serum insulin levels of wild-type (■) and transgenic (▨) mice under a normal or high-fat

immunostained sections using OctA-Probe (D-8) (sc-807; Santa Cruz Biotechnology). After washing with PBS, we incubated the sections sequentially with biotinylated anti-rabbit IgG reagent (Vector Laboratories) and Vectastain Elite ABC reagent (Vector Laboratories) and visualized with the Liquid DAB Substrate Chromogen System (DakoCytomation). For histological analysis, we removed interscapular tissue from 15-week high-fat–dieted mice, fixed the specimens in 10% paraformaldehyde, and embedded them in paraffin. We mounted consecutive 10-μm sections on slides and stained them with hematoxylin and eosin. We calculated adipose cell size with NIH Image 1.62 software by manual tracing of at least 500 adipocytes for each genotype. Measurement of the size of adipocytes in WAT was performed using FLVFS-LS software (Flovel, Tokyo, Japan) by manual tracing of at least 500 adipocytes for each genotype.

Fractionation of cytoplasmic and nuclear proteins of BAT. After treatment with 1 mg/ml of collagenase I (Roche), cytoplasmic and nuclear extracts of 150 μg of BAT tissues from wild-type and transgenic mice were fractionated by differential lysis of cells in two consecutive steps using the NE-PER extraction reagents (Pierce). Protein concentrations in the cytoplasmic and nuclear extracts were determined using the Micro BSA protein assay kit (Pierce), and aliquots (30 μg) were resolved on 8 or 14% SDS-PAGE, followed by Western blotting using the indicated antibodies.

Culture of a brown adipocyte cell line, T37i cells, and infection with adenoviruses encoding FoxO1. T37i cells were cultured in Dulbecco's modified Eagle's medium–Ham's F12 medium (Invitrogen) supplemented with 10% FCS, 2 mmol/l glutamine, 100 IU/ml penicillin, 100 μg/ml streptomycin, and 20 mmol/l HEPES and were grown at 37°C in a humidified atmosphere with 5% CO_2. Differentiation into mature adipocytes was achieved under standard conditions by incubating subconfluent undifferentiated T37i cells with 2 nmol/l triiodothyronine (T3; Sigma Chemical, St. Louis, MO) and 20 nmol/l insulin (Invitrogen) for 6 days. Construction of adenoviruses encoding FoxO1 mutants was described elsewhere (18). For infection with adenoviruses, after differentiation into mature adipocytes, cells were infected with adenoviruses at multiplicity of infections between 10 and 20. At 72 h after infection, cells were harvested.

Knockdown of endogenous FoxO1 in T37i cells. We used RNAi-Ready pSIREN-Shuttle vector (Clontech) with GCTGCAGTACTCTCCTTATGG as the target sequence and selected target sequence of FoxO1 by Block-iT RNAi Designer (Invitrogen). We generated scrambled control plasmid using mismatch sequence GC***G***GCAGTACTC***C***CCTTA***G***GG. After transfection of cells with the knockdown vector using Lipofectamine (Invitrogen), cells were induced by differentiation medium. At day 5 after induction, cells were harvested and real-time PCR or Western blotting was performed.

Statistical analyses. We calculated descriptive statistics using ANOVA followed by Fisher's test (Statview; SAS Institute). P values of <0.05 were considered significant.

RESULTS

Generation of adipose tissue–specific mutant FoxO1 transgenic mice. It has been already reported that FoxO family members (*FoxO*s) were expressed in both WAT and BAT and that haploinsufficiency of *FoxO1* altered histological appearance and gene expression in WAT (17). However, it is not known whether FoxO1 has some physiological roles in mature adipose tissues, especially in BAT. To investigate roles of FoxO1 in adipose tissue, we generated adipose tissue–specific *FoxO1* transgenic mice *(aP_2-FLAG-Δ256)* using an adipose tissue–specific 5.4-kb promoter/enhancer fragment of the mouse *aP_2*, also called fatty acid binding protein 4 (*FABP4*), and a FLAG-tagged mutant FoxO1 (FLAGΔ256), which lacks carboxyl terminal transactivation domain (18) (Fig. 1*A*). It has been reported that *aP_2* promoter was active in WAT and/or BAT (23–25) and that the FLAGΔ256 can compete with endogenous FoxOs and inhibit expression of FoxOs' target genes (26). We generated two transgenic lines in which FLAGΔ256 was expressed mainly in BAT under the normal-diet condition (Fig. 1*B*). Transgene expression level in BAT in line 2 was more pronounced than in line 1 (Fig. 1*B*, *lanes 2* and *4*). The FLAGΔ256 mRNA in line 2 was expressed in adipose tissue, especially BAT (Fig. 1*C*, *lane 2*). The FLAGΔ256 protein was also expressed to a greater extent in BAT than in WAT in both lines (Fig. 1*D*). Finally, we examined intracellular localization of FLAGΔ256 in BAT from line 2 and detected a nuclear staining of the FLAGΔ256 in BAT from line 2 (Fig. 1*E*). In BAT, under a normal diet, endogenous FoxO1 is phosphorylated (Fig. 1*F*, *lanes 1* and *2*) and localized both in cytosol and in the nucleus (Fig. 1*G*, *upper panel*). However, on the high-fat diet, phosphorylation of endogenous FoxO1 is decreased (Fig. 1*F*, *lanes 3* and *4*) and FoxO1 is localized mainly in the nucleus (Fig. 1*G*, *upper panel*). In contrast, the FLAGΔ256 is localized constitutively in the nucleus in both the normal and high-fat diets (Fig. 1*G*, *middle panel)*. Therefore, the FLAGΔ256 may compete with endogenous FoxOs and inhibit their transcriptional activity on promoter regions of their target genes in BAT. For subsequent analyses, we used line 2, which has a higher transgene expression levels in BAT than line 1.

Improved insulin sensitivity in adipose tissue–specific FoxO1 transgenic mice. To investigate the functional consequences of FLAGΔ256 overexpression in adipose tissue on glucose metabolism and energy homeostasis, we measured body weight, blood glucose, and serum insulin levels and performed intraperitoneal glucose and insulin tolerance tests. The *aP_2-FLAG-Δ256* mice have a tendency to have reduced body weight under the normal diet. Especially, from 12 to 14 weeks of age, they showed statistically significant lower body weight than wild-type mice (Fig. 2*A*). At the age of 3 months, *aP_2-*

diet. Data represent means ± SE of 15 male mice for each genotype. *Statistically significant difference between wild-type and transgenic mice ($P < 0.005$ by one-factor ANOVA). *D*: Western blotting of endogenous phosphorylated FoxO1 in WAT from wild-type mice under a normal diet (*lanes 1* and *2*) and a high-fat diet (*lanes 3* and *4*). The *top panel* shows Western blotting of phosphorylated FoxO1 with anti-pT24, the *middle panel* shows Western blotting of total FoxO1 with anti-FOXO1 (N18), and the *bottom panel* shows Western blotting of tubulin. *E*: Tissue survey of transgene expression in transgenic mice under a 15-week high-fat diet. Total RNA was isolated from the tissues indicated at the bottom of the autoradiogram and analyzed by Northern blotting using a *FoxO1* and *Actin* cDNA probe. *F*: Real-time PCR of transgene expression in WAT (■) and BAT (▨) under a normal or high-fat diet. The relative mRNA abundance of transgene is shown as folds of expression levels of transgene in WAT under a normal diet. Data represent means ± SE of RNA samples from five transgenic mice for each tissue. *Statistically significant difference between WAT under a normal or high-fat diet ($P < 0.005$ by one-factor ANOVA). The primers used in genotyping, FLAG-S1 and SE1AS, were used for this real-time PCR. *G*: The transgene is expressed in WAT as well as BAT under a 15-week high-fat–dieted condition. Lysates from WAT (*lanes 1–6*) and BAT (*lanes 7–12*) of wild-type (*lanes 1–3* and *6–9*) and transgenic (*lanes 4–6* and *10–12*) mice were electrophoresed and immunoblotted with the indicated antibodies. An arrow (*upper band*) indicates FLAG-Δ256, and an asterisk (*lower band*) indicates a nonspecific band. *H*: Immunohistochemistry of WAT from wild-type (*left panel*) and transgenic (*right panel*) mice. Scale bars indicate 20 μm. *I*: Intraperitoneal glucose tolerance test in transgenic mice under a high-fat diet ($n = 10$ for each genotype). ○, wild-type mice; ●, transgenic mice. *Statistically significant differences between wild-type and transgenic mice ($P < 0.05$ by one-factor ANOVA). *J*: Intraperitoneal insulin tolerance test in transgenic mice under a high-fat diet ($n = 10$ for each genotype). *Statistically significant difference between wild-type and transgenic mice ($P < 0.05$ by one-factor ANOVA). ○, wild-type mice; ●, transgenic mice. *K* and *L*: Real-time PCR of *G6pc* and *Pck1* using liver from wild-type (■) and transgenic (▨) mice under a normal diet (*K*) or high-fat diet (*L*). Data represent means ± SE of RNA samples from five transgenic mice at fasting state. A single or double asterisk indicates a statistically significant difference of *G6pc* expression between wild-type and transgenic mice (*$P < 0.01$ and **$P < 0.05$ by one-factor ANOVA). Primers for real-time PCR of *G6pc* and *Pck1* were described elsewhere (22). *M*: Hepatic glycogen content of wild-type (■) and transgenic (▨) mice under normal and high-fat diets in the fasting state.

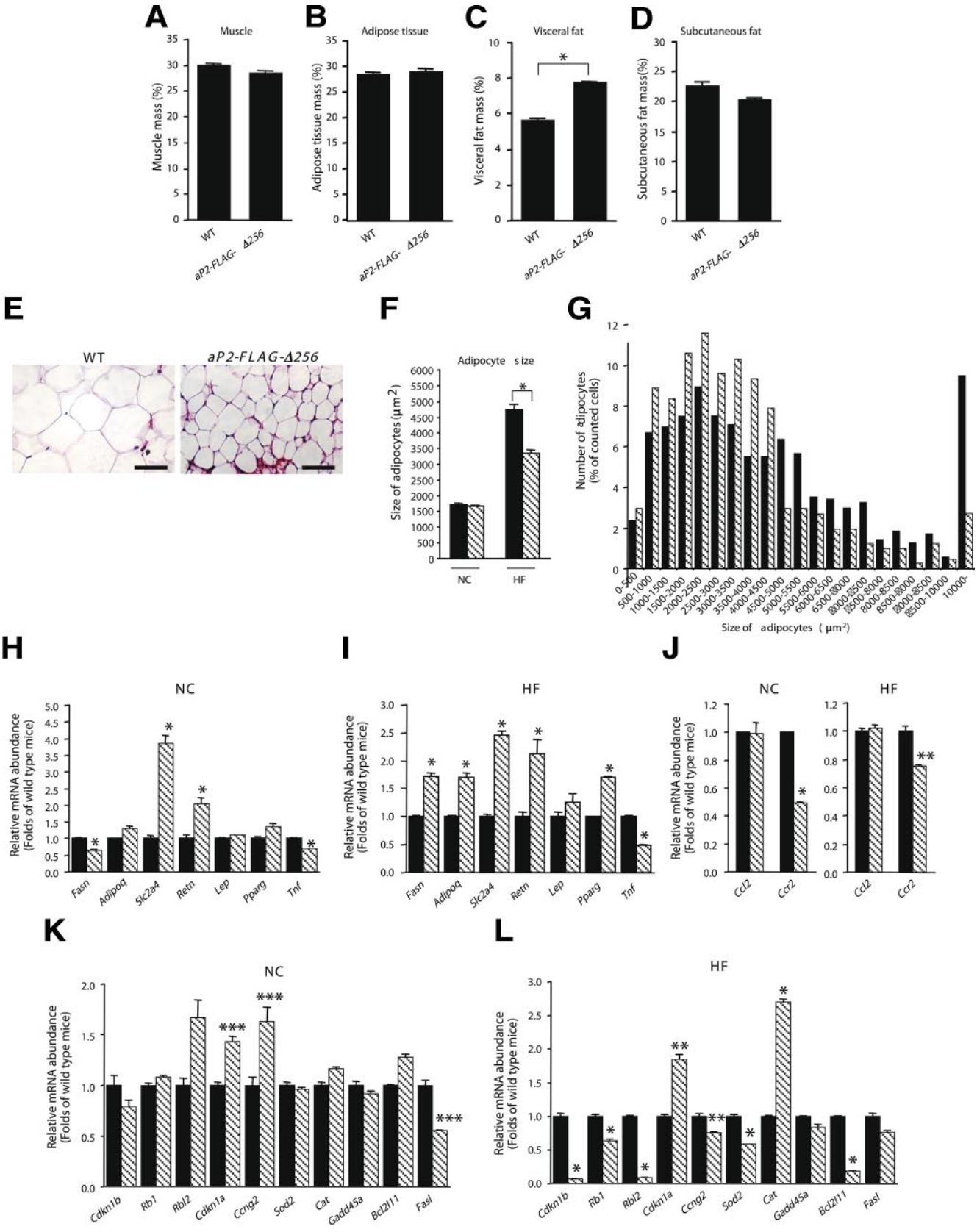

FIG. 3. Adiposity, histological analyses, and gene expression of WAT from transgenic mice. Muscle mass (*A*), adipose tissue mass (sum of visceral and subcutaneous fats) (*B*), visceral fat mass (*C*), and subcutaneous fat mass (*D*) were calculated as described in RESEARCH DESIGN AND METHODS. The data are demonstrated as percent of body weight and represented as means ± SE from five mice of each genotype. *Statistically significant difference of visceral fat mass between wild-type and transgenic mice (P* < 0.01 by one-factor ANOVA). *E*: Histological appearance of WAT from wild-type (*left panel*) and transgenic (*right panel*) mice. Sections were stained with hematoxylin and eosin. Representative photomicrographs are presented. Scale bars indicate 100 μm. *F*: Average of size of adipocytes from epididymal fat of wild-type (■) and transgenic (▨) mice under normal-diet (NC) and high-fat diet (HF) conditions. *Statistically significant difference between wild-type and transgenic mice under a high-fat**

FLAG-Δ256 had no significant differences of fed blood glucose and serum insulin levels compared with wild-type mice (data not shown). The intraperitoneal glucose tolerance test, insulin secretion, and the insulin tolerance test did not show any significant differences between wild-type and *aP$_2$-FLAG-Δ256* mice (data not shown). At the age of 6 months, although body weight and fed blood glucose levels of *aP$_2$-FLAG-Δ256* were not different from wild-type mice, fed serum insulin levels of *aP$_2$-FLAG-Δ256* were significantly lower than wild-type mice (Fig. 2*B* and *C*). An intraperitoneal glucose tolerance test demonstrated that *aP$_2$-FLAG-Δ256* tended to be more glucose tolerant compared with wild-type mice, but it did not reach statistical significance (online appendix Fig. 1*A*). However, insulin secretion during the intraperitoneal glucose tolerance test in *aP$_2$-FLAG-Δ256* was significantly lower than in wild-type mice (online appendix Fig. 1*B*). Insulin tolerance test did not show any significant difference between *aP$_2$-FLAG-Δ256* and wild-type mice (data not shown).

Next, in order to clarify whether the FLAGΔ256 overexpression in adipose tissue may affect glucose metabolism and energy homeostasis, *aP$_2$-FLAG-Δ256* and wild-type mice were fed a high-fat diet for 15 weeks after weaning. Western blotting of endogenous FoxO1 in WAT demonstrated that FoxO1 is phosphorylated under normal diet, but under the high-fat–dieted condition, FoxO1 is dephosphorylated (Fig. 2*D*). Interestingly, a 15-week high-fat diet induced transgene expression in WAT as well as in BAT (Fig. 2*E* and *F*). Real-time PCR revealed that transgene expression in WAT under a high-fat diet increased by fivefold compared with under a normal diet (Fig. 2*F*). Consistent with the gene expression level of transgene, Western blotting demonstrated that FLAGΔ256 protein could be detected in WAT as well as in BAT (Fig. 2*G*). Immunohistochemistry showed that the FLAGΔ256 was mainly expressed in the nucleus of white adipocytes (Fig. 2*H*). Body weight was not different from wild-type mice (Fig. 2*A*). However, fed blood glucose levels of transgenic mice were significantly lower than wild-type mice (Fig. 2*B*), and serum insulin levels of transgenic mice tended to be lower than wild-type mice, but it was not statistically significant (Fig. 2*C*). Food intake and serum leptin level in *aP$_2$-FLAG-Δ256* were not different from wild-type mice both under the normal and high-fat–dieted condition (online appendix Fig. 2). Fasting blood glucose levels of transgenic mice were significantly lower than wild-type mice and an intraperitoneal glucose tolerance test demonstrated that *aP$_2$-FLAG-Δ256* were significantly more glucose tolerant than wild-type mice (Fig. 2*I*). An insulin tolerance test also demonstrated that insulin sensitivity of *aP$_2$-FLAG-Δ256* was improved significantly compared with wild-type mice (Fig. 2*J*). To assess hepatic glucose production indirectly, we examined gene expression levels of *G6Pase* (*G6pc*) and *Pepck* (*Pck1*), which are involved in gluconeogenesis, and measured hepatic glycogen content. In both the normal and high-fat diet, although hepatic *G6pc* expression in *aP$_2$-FLAG-Δ256* was significantly decreased compared with wild-type mice, *Pck1* expression was not changed (Fig. 2*K* and *L*). However, the hepatic glycogen content of *aP$_2$-FLAG-Δ256* was not different from wild-type mice (Fig. 2*M*). These data suggest that overexpression of FLAGΔ256 in adipose tissue ameliorates insulin resistance induced by a high-fat diet.

Overexpression of the mutant FoxO1 in WAT affects size and gene expression of white adipocytes. To investigate the mechanism of how FLAGΔ256 improves glucose tolerance and insulin sensitivity, we examined adiposity, histological analyses, and gene expression in WAT. Computed tomography scanning revealed that visceral fat mass was increased significantly and subcutaneous fat mass of transgenic mice was decreased slightly compared with wild-type mice under a high-fat diet condition, although muscle and whole adipose tissue mass of transgenic mice were not changed (Fig. 3*A–D*). Interestingly, histological analyses of epididymal fat demonstrated that the size of adipocytes from transgenic mice was significantly smaller than wild-type mice (Fig. 3*E–G*). We performed real-time PCR in order to investigate the effects of FLAGΔ256 on gene expression of WAT-specific metabolic and inflammatory genes. Under a normal diet, *Slc2a4* and *resistin* (*Retn*) gene expression levels were increased and *fatty acid synthase* (*Fasn*) and *tumor necrosis factor* (*Tnf*) gene expression levels in WAT from transgenic mice were significantly decreased compared with wild-type mice (Fig. 3*H*). Furthermore, in WAT from transgenic mice under a high-fat diet, *Fasn*, *adiponectin*, *Scl2a4*, *Retn*, and *Pparγ* (*Pparg*) gene expression levels were increased, but *Tnf* gene expression was significantly suppressed (Fig. 3*I*). Serum resistin concentration of transgenic mice was not different from wild-type mice (online appendix Fig. 3). In addition, the expression level of chemokine (C-C motif) receptor 2 (*Ccr2*), a receptor for monocyte chemoattractant protein modulating metabolic and inflammatory effects induced by a high-fat diet (27), was significantly decreased in WAT from transgenic mice under both normal and high-fat diet and was significantly decreased compared with wild-type mice (Fig. 3*J*). These data suggest that overexpression of a mutant FoxO1 affects adipocyte size and gene expression in WAT.

Effects of a mutant FoxO1 on gene expression of FoxO target genes in WAT. It has been reported that FoxOs have various classes of target genes, which are involved in apoptosis, regulation of cell cycle, stress resistance, and DNA repair, other than glucose metabolism (28) and a constitutively nuclear FoxO1 (T24A/S253D/5316A)-inhibited adipocyte differentiation. Therefore, we hypothesized that overexpression of FLAGΔ256 in WAT may affect gene expression of FoxO target genes and adipocyte differentiation and finally affect adipocyte size and the examined gene expression

diet (*P < 0.001 by one-factor ANOVA). *G*: Distribution of sizes of adipocytes. Sizes of each adipocyte from wild-type (■) or transgenic (▨) mice under a high-fat diet were measured as described in RESEARCH DESIGN AND METHODS. The data represent percent of adipocytes with each size among all measured cell number. Real-time PCR of WAT-specific genes using WAT from wild-type (■) and transgenic (▨) mice under normal (NC) (*H*) or high-fat (HF) diet (*I*). Data represent means ± SE of RNA samples from each of the five genotypes. *Statistically significant difference between wild-type and transgenic mice (*P < 0.01 by one-factor ANOVA). *J*: Real-time PCR of *Ccl2* and *Ccr2* using WAT from wild-type (■) and transgenic (▨) mice under a normal diet (*left panel*) or high-fat (*right panel*) diet. Data represent means ± SE of RNA samples from each of the five genotypes. A single or double asterisk indicates a statistically significant difference between wild-type and transgenic mice (*P < 0.01 and **P < 0.05 by one-factor ANOVA). Real-time PCR of FoxO1 target genes using WAT from wild-type (■) and transgenic (▨) mice under a normal diet (*K*) or high-fat diet (*L*). Data represent means ± SE of RNA samples from each of the five genotypes. A single, double, or triple asterisk indicates a statistically significant difference between wild-type and transgenic mice (*P < 0.001, **P < 0.005, and ***P < 0.01 by one-factor ANOVA).

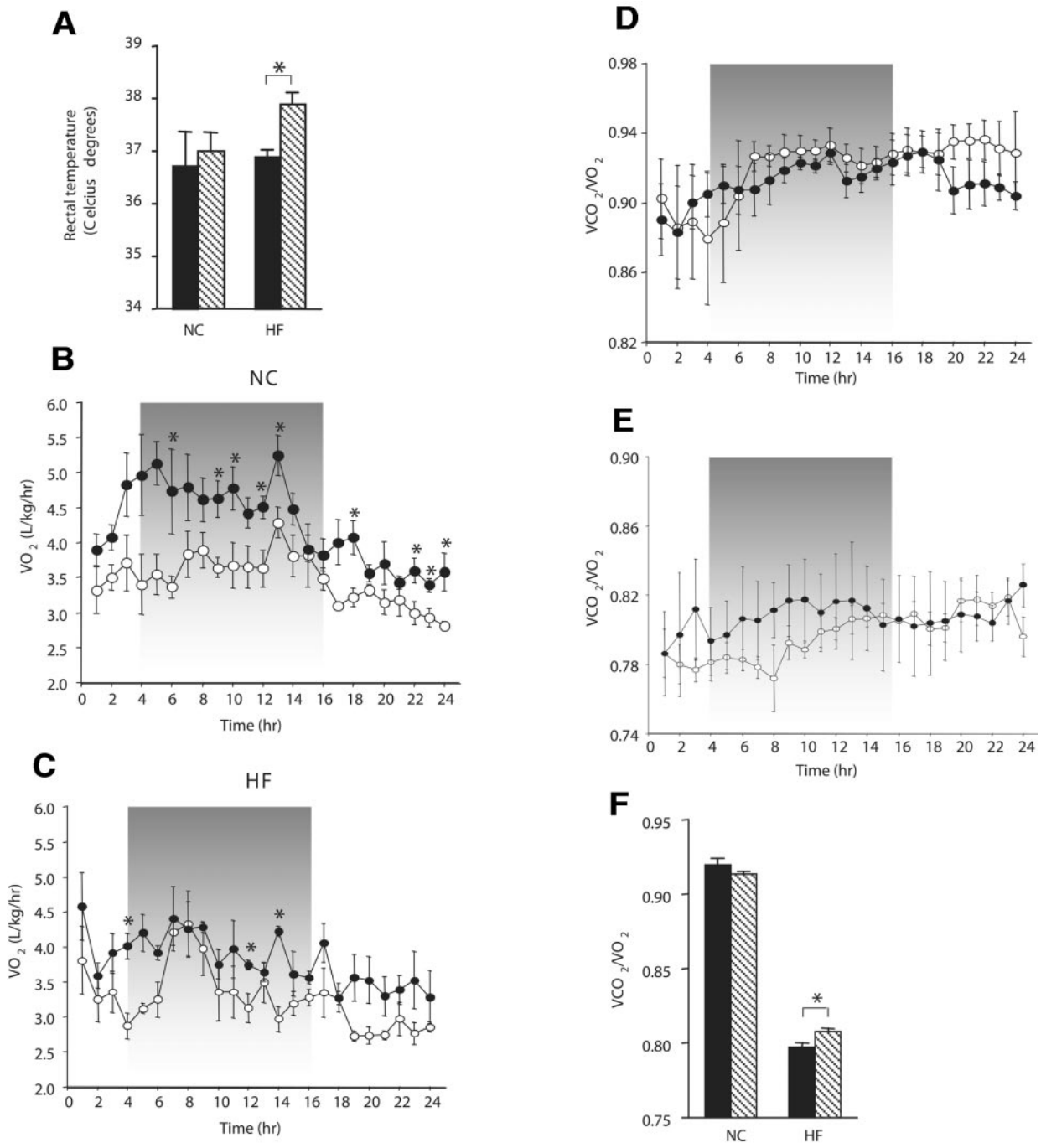

FIG. 4. Body temperature and metabolic rates of transgenic mice. *A*: Rectal temperature of 6-month-old male mice (five for each genotype) under a normal diet (NC) and 15-week high-fat–dieted (HF) male mice (five for each genotype) were measured at room temperature. ■, wild-type mice; ▧, transgenic mice. *Statistically significant difference between wild-type and transgenic mice under a high-fat–dieted condition ($P < 0.01$ by one-factor ANOVA). *B* and *C*: The oxygen consumption of wild-type and transgenic mice under a normal diet (NC) at the age of 6 months or under a 15-week high-fat diet (HF). The data represented were means ± SE of five male mice for each genotype and each condition. Measurements of oxygen consumption were performed for 72 h, with the first day allowing the mice to acclimate to the cage environment. ○, wild-type mice; ●, transgenic mice. The dark shadow indicates the dark phase. *Statistically significant differences between wild-type and transgenic mice (*$P < 0.02$ by one-factor ANOVA). *D* and *E*: Respiratory quotient of wild-type and transgenic mice. The data represented were means ± SE of five male mice for each genotype and each condition as described in Fig. 4*B* and *C*. ○, wild-type; ●, transgenic mice. The dark shadow indicates the dark phase. *F*: Average of respiratory quotient from Fig. 4*D* and *E*. ■, wild-type mice; ▧, transgenic mice under a normal or high-fat diet. *Statistically significant difference between wild-type and transgenic mice under a high-fat diet (*$P < 0.05$ by one-factor ANOVA).

of FoxO target genes. It can be speculated that gene expression levels of typical FoxO target genes should be suppressed by the FLAGΔ256. Interestingly, in WAT from *aP$_2$-FLAG-Δ256* under a norma diet, gene expression levels of most FoxO1 target genes except *p21* (*Cdkn1a*), *Cyclin G2* (*Ccng2*), and *Fas ligand* (*Fasl*) were not affected (Fig. 3*K*). However, under a high-fat diet, gene expression levels of most FoxO1 target genes, except *Cdkn1a* and *Catalase* (*Cat*), were suppressed (Fig. 3*L*). These data suggest that overexpression of FLAGΔ256 under a high-fat diet affects the size of adipocytes and gene expression in WAT.

Increased energy expenditure by overexpression of mutant FoxO1 in BAT. To investigate effects of overexpression of FLAGΔ256 on the physiological function of BAT, we measured resting rectal temperature. Although rectal temperature in *aP$_2$-FLAG-Δ256* was similar to wild-type mice under a normal diet, rectal temperature under a high-fat diet was significantly higher than wild-type mice (Fig. 4*A*). Furthermore, oxygen consumption was measured using indirect calorimetry. Oxygen consumption of *aP$_2$-FLAG-Δ256* was significantly higher than wild-type mice under both normal and high-fat diet conditions (Fig. 4*B* and *C*). Respiratory quotient, which represents utilization of carbohydrate or fat for a fuel source, of *aP$_2$-FLAG-Δ256* was similar to wild-type mice under a normal diet (Fig. 4*D* and *F*). However, under a high-fat diet, the respiratory quotient of *aP$_2$-FLAG-Δ256* tended to be higher than wild-type mice, especially in the dark state (Fig. 4*E*), and the average of the respiratory quotient of *aP$_2$-FLAG-Δ256* was also significantly higher than wild-type mice (Fig. 4*F*). These data indicate that overexpression of the FLAGΔ256 in BAT increases oxygen consumption and energy expenditure and may reflect increased carbohydrate utilization, which spared triglyceride oxidation and stimulated the accumulation of adipose tissue.

Overexpression of mutant FoxO1 in BAT increases the number of brown adipocytes. To investigate the effects of overexpression of FLAGΔ256 on BAT, we measured weights of BAT and investigated histological appearance of BAT from wild-type and transgenic mice under a high-fat diet. Weights of BAT in *aP$_2$-FLAG-Δ256* under a normal diet were not different compared with wild-type mice (data not shown). Furthermore, we could not detect any significant difference in weights of BAT in *aP$_2$-FLAG-Δ256* under a high fat-diet compared with wild-type mice (Fig. 5*A*). However, numbers of brown adipocytes in BAT from *aP$_2$-FLAG-Δ256* were increased significantly compared with wild-type mice (Fig. 5*B* and *C*). These data suggest that overexpression of FLAGΔ256 apparently affects the morphological appearance of brown adipocytes and reverses the histological phenotype of BAT induced by a high-fat diet.

Pleiotropic effects of mutant FoxO1 on gene and protein expression in BAT. To investigate effects of the FLAGΔ256 on BAT-specific gene expression, we performed real-time PCR using total RNA of BAT from wild-type and *aP$_2$-FLAG-Δ256* mice under a normal or high-fat diet condition. Under a normal diet, overexpression of FLAGΔ256 in BAT increased *Ppargc1b*, *Ucp1*, and*Ucp2* gene expression significantly compared with wild-type mice (Fig. 5*D*). Furthermore, in BAT from *aP$_2$-FLAG-Δ256* mice under a high-fat diet, *Ppargc1b*, *Ucp1*, *Ucp2*, and*Adrb3*, which have important roles in BAT function, gene expression levels were significantly increased compared with wild-type mice (Fig. 5*E*). In contrast, under the high-fat diet, overexpression of FLAGΔ256 in BAT significantly decreased *4ebp-1* (*Eif4ebp1*) gene expression (Fig. 5*E*). The *Eif4ebp1*gene has been reported to be a target gene of dFOXO in *Drosophila* (29,30) and in mice (31). Therefore, it can be speculated that the FLAGΔ256 suppresses *Eif4ebp1* gene expression in BAT. *Ppargc1a* gene expression under a high-fat diet was decreased but not statistically significantly. These data suggest that overexpression of FLAGΔ256 in BAT affects gene expression and may ameliorate BAT function under a high-fat–dieted condition.

It has been reported that targeted disruption of *Eif4ebp1* caused increased translation of PGC-1 protein (32). Therefore, it is worth it to investigate PGC-1α protein levels in BAT from *aP$_2$-FLAG-Δ256* mice. To examine whether overexpression of FLAGΔ256 in BAT may affect PGC-1α protein expression levels, we performed Western blotting using lysates of BAT from wild-type and *aP$_2$-FLAG-Δ256* mice under a normal or high-fat–dieted condition. In the normal-diet condition, PGC-1α, 4E-BP1, and UCP-1 protein levels in BAT from *aP$_2$-FLAG-Δ256* tended to be higher, but these effects were not statistically significant (Fig. 5*F* and *G*). However, in the high-fat diet, PGC-1α protein levels were increased and 4E-BP1protein levels were decreased significantly compared with wild-type mice (Fig. 5*F* and *H*). UCP-1 protein levels in BAT from *aP$_2$-FLAG-Δ256* was also increased but not statistically significantly (Fig. 5*F* and *H*). These data indicate that overexpression of FLAGΔ256 in BAT increases PGC-1α protein expression levels under a high-fat diet. Consistent with the findings above, overexpression of FLAGΔ256 in BAT increased gene expression levels for many genes of mitochondrial oxidative phosphorylation that are known to be enriched in BAT, which include *Cox5b*, *CoxIII*, *Cox8b*, *Cox4i1*, and cytochrome c (*Cyc*) (33), in both normal and high-fat–dieted conditions (Fig. 5*I* and *J*). These data suggest that overexpression of FLAGΔ256 increases mitochondrial gene expression and finally may upregulate physiological function of BAT.

The mutant FoxO1 increased *Ucp1* and *Adrb3* gene expression levels in the T37i cell line. To confirm whether the FLAGΔ256 in BAT increases PGC-1α expression levels and endows BAT-specific phenotypes on cells, we infected differentiated T37i cells with adenovirus encoding LacZ and constitutively nuclear (CN) or Δ256 FoxO1 and analyzed gene expression. T37i cells are derived from the hibernoma of SV40 large T antigen transgenic mice under the control of human mineralocorticoid receptor promoter. T37i cells maintain the ability to undergo terminal differentiation and remain capable of expressing *Ucp1* upon retinoic acid and β-adrenergic stimulation (34,35). After T37i cells were differentiated into mature brown adipocytes, we infected cells with adenovirus encoding FoxO1 (Fig. 6*B*). We used adenoviruses encoding ADA FoxO1 as CN mutant and Δ256 FoxO1 (18). At day 3 after infection, we harvested cells and performed real-time PCR. Overexpression of the CN FoxO1 increased *Eif4ebp1* and *Ppargc1a* gene expression significantly (Fig. 6*A*). In contrast, *Eif4ebp1* and *Ppargc1a* gene expression levels in cells infected with the Δ256 FoxO1 were not changed compared with the LacZ-infected cells (Fig. 6*A*). However, although overexpression of the CN FoxO1 did not affect 4E-BP1 and PGC-1α protein levels, overexpression of the Δ256 FoxO1 in cells decreased 4E-BP1 protein levels and increased PGC-1α protein levels (Fig. 6*B*). Furthermore, overexpression of the Δ256 FoxO1 increased *Ucp1* and *Adrb3* gene expression in T37i cells (Fig. 6*A*). These data indicate that inhibition of transcriptional activity FoxO1 in T37i cells increases PGC-1α protein and *Ucp1* and *Adrb3* gene expression levels.

Knockdown of FoxO1 in T37i cells enhances BAT-specific gene expression. Because the truncated FoxO1 used in the present study lacks the COOH-terminal transactivation domain but retains the NH_2-terminal and forkhead DNA binding domain, it is possible that this mutant FoxO1 may affect functions of other Fox proteins, includ-

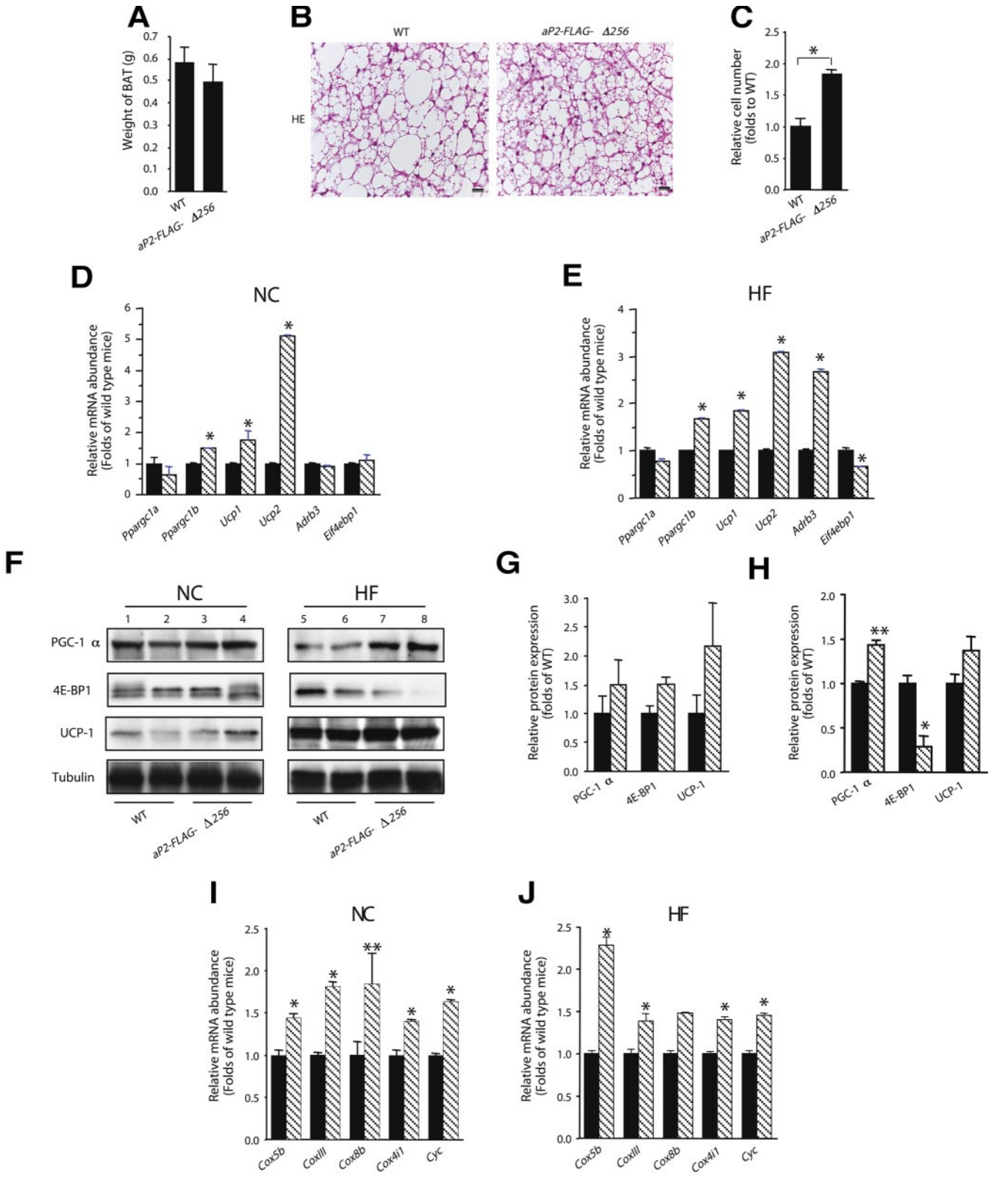

FIG. 5. Effects of the mutant FoxO1 on histological appearance and gene and protein expression in BAT. *A*: Weights of BAT from wild-type and transgenic mice under a high-fat–dieted condition for 15 weeks. The data presented are means ± SE of the weight of BAT from each genotype (n = 8 for each genotype). *B*: Histological appearance of BAT from wild-type (*left panel*) and transgenic (*right panel*) mice under a 15-week high-fat diet. Interscapular tissue was excised and fixed. Sections were stained with hematoxylin and eosin. Representative photomicrographs are presented. Scale bars indicate 20 μm. *C*: The number of fat cells within a random microscopic field was determined by counting cells in at least six different random fields per mouse and six mice for each genotype. The data are means ± SE and represented as folds of data of wild-type mice. *Statistically significant difference (P < 0.005 by one-factor ANOVA). Real-time PCR of genes that are expressed in BAT of wild-type and transgenic mice at the age of 6 months under normal diet (NC) (*D*) or 15-week high-fat diet (HF) (*E*). Isolation of total RNA and real-time PCR was performed as described in RESEARCH DESIGN AND METHODS. ■, wild-type mice; ▨, transgenic mice. The data presented are means ± SE of three independent experiments (n = 4 for each genotype and each condition). *Statistically significant differences between wild-type and

ing FoxC2 and FoxA2 (36,37) and have effects on some FoxO-binding proteins, such as Sirt1 and PGC-1α (15,38). The best way to elucidate physiological roles of FoxO1 in adipose tissue may be the generation of adipose tissue–specific FoxO1 knockout mice. However, at the present time, we could not generate them. Therefore, we tried to investigate physiological roles of FoxO1 in T37i cells using short-hairpin RNA (shRNA). Transfection with shRNA was performed at the same day as the induction of adipocyte differentiation, and cells were harvested at day 5 after induction. Expression of shRNA reduced expression of FoxO1 by ~80% (Fig. 6*C*, *left panel*, and *D*). In contrast, other FoxOs, which include FoxO3a and FoxO4, gene expression levels were increased significantly compared with cells transfected with a scrambled control shRNA (Fig. 6*C*, *right panel*). Knockdown of endogenous FoxO1 increased gene expression levels of Ppargc1a, Ppargc1b, Ucp1, and Adrb3 significantly and increased UCP-1 protein expression in the presence of isoproterenol (Fig. 6*D* and *E*). Pparg gene expression in shRNA-transfected cells increased significantly, and Eif4ebp1 gene expression levels were not changed compared with scrambled control–transfected cells (Fig. 6*E*). These data demonstrate that knockdown of FoxO1 confers the molecular phenotype of BAT cells onto T37i cells.

DISCUSSION

In the present study, we generated two lines of adipose tissue–specific mutant FoxO1 transgenic mice (*aP_2-FLAG-Δ256*) using an adipose tissue–specific 5.4-kb promoter/enhancer fragment of the mouse *aP_2* gene. In both lines, FLAGΔ256 is expressed in BAT much more than WAT under a normal diet. The *aP_2-FLAG-Δ256* showed improved glucose tolerance and insulin sensitivity under a high-fat diet. Overexpression of FLAGΔ256 in WAT lead to increased visceral fat mass, increased small adipocytes, and altered expression levels of adipose tissue–related genes, such as *Fasn*, *adiponectin*, *Slc2a4*, *Retn*, *Pparg*, *Tnf*, and *Ccr2*. Furthermore, overexpression of FLAGΔ256 in BAT leads to increased oxygen consumption accompanied with increased expression of PGC-1α, *Ucp1*, and *Adrb3*.

Interestingly, in the present study, a high-fat diet increased the expression level of FLAGΔ256 in WAT as well as BAT. Because it has been reported that a high-fat diet induced *aP2* gene expression and content (39), it can be speculated that a high-fat diet activated *aP2* promoter used in this study and induced transgene expression in WAT. Under a high-fat diet, phosphorylation of endogenous FoxO1 is decreased in adipose tissue. FLAGΔ256 in WAT and BAT from transgenic mice was also present in nucleus. Therefore, it can compete with endogenous FoxOs and inhibit their transcriptional activity. Indeed, expression levels of several FoxO1 target genes, which include *p27* (*Cdkn1b*) (40), *pRb* (*Rb1*) (17), *p130* (*Rbl2*) (41), *Ccng2* (42), *MnSod* (*Sod2*) (43), and *Bim (Bcl2l11*) (44), were suppressed in WAT. The effects of overexpression of FLAGΔ256 on glucose tolerance and insulin sensitivity under a normal diet were smaller than under a high-fat diet. These can be explained by the findings that endogenous FoxO1 in adipose tissues under a normal diet is phosphorylated and overexpression of the FLAGΔ256 did not result in significant alterations in adipocytic gene expression in adipose tissue under a normal diet. However, under a high-fat diet, endogenous FoxO1 is dephosphorylated and may activate expression of its target genes. In that circumstance, the FLAGΔ256 can inhibit expression of FoxOs' target genes and normalize glucose tolerance, insulin sensitivity, and oxygen consumption.

The *aP_2-FLAG-Δ256* mice showed increased expression of PGC-1α protein, which is a key coactivator for adaptive thermogenesis in BAT (9), and increased expression of the *Ucp1* gene, body temperature, and oxygen consumption. It has been known that d4E-BP is one of the target genes of dFOXO in *Drosophila* (29), and recently it has been reported that *Eif4ebp1* is a target gene of FoxO1 in C2C12 cells (31). Furthermore, *Eif4ebp1*$^{-/-}$ mice exhibited smaller WAT and an increased metabolic rate due to increased expression of PGC-1α, *Ucp1*, and *Adrb3* in WAT, although the mechanism whereby reduced expression of 4E-BP1 leads to enhanced expression of PGC-1α remains to be elucidated (32). Several genes that are involved in mitochondrial oxidative phosphorylation and are known to be enriched in BAT from transgenic mice were increased. Therefore, it is speculated that FLAGΔ256 in BAT may inhibit *Eif4ebp1*expression and increases PGC-1α protein expression through an unknown mechanism and drives the molecular phenotype of BAT. However, at cellular levels, we could not detect any significant differences of expression levels of *Eif4ebp1* between LacZ- and Δ256-infected cells. This discrepancy has been shown by another study (45) that the same Δ256 FoxO1 increased *adipoq* expression, although it was shown to be a target gene of FoxO1. One of the possibilities might be that FLAGΔ256 used in the present study still had the NH_2-terminus and forkhead DNA binding domain and these domains could bind to some cofactors for transcription of FoxO1 target genes in a tissue-specific or cell type–specific manner. Using knockdown of endogenous FoxO1 by shRNA, we could demonstrate that ~80% knockdown of endogenous FoxO1 in T37i cells enhanced the molecular phenotype of brown adipocytes through increased expression of *Ppargc1a*, *Ppargc1b*, *Ucp1*, and *Adrb3*. These data suggest that FoxO1 may suppress gene expression of BAT-specific genes and also suggest the possibility that FoxO1 could affect differentiation of T37i cells into mature brown adipocytes as well as the previous report that CN FoxO1 inhibits differentiation of white preadipocyte cell line 3T3-F442A cells (17) because *Pparg* expression in T37i cells transfected with sh-FoxO1 vector was increased

transgenic mice (*P < 0.001 by one-factor ANOVA). *F*: Western blotting of PGC-1α, 4E-BP1, and UCP-1 proteins in BAT from wild-type and transgenic mice at the age of 6 months (NC) or 15-week high-fat diet (HF). Tissue lysates (50 μg) of BAT from wild-type (*lanes 1*, *2*, *5*, and *6*) and transgenic (*lanes 3*, *4*, *7*, and *8*) mice under the normal diet (*left panel*) or high-fat–dieted condition (*right panel*) were electrophoresed in SDS-PAGE and immunoblotted with the indicated antibodies. Quantitative analyses of PGC-1α, 4E-BP1, and UCP-1 protein expression levels in BAT from wild-type (■) and transgenic (▨) mice at the age of 6 months under normal-diet (*G*) or high-fat diet (*H*) conditions. Intensity of bands blotted with anti–PGC-1α, −4E-BP1, and –UCP-1 was measured using NIH Image 1.62. Data represent means ± SE from three independent experiments. *Statistically significant differences between wild-type and transgenic mice (*P < 0.01 and **P < 0.02 by one-factor ANOVA). Real-time PCR of genes of mitochondrial components in BAT of wild-type and transgenic mice at the age of 6 months under normal diet (NC) (*I*) or 15-week high-fat diet (*J*). ■, wild-type mice; ▨, transgenic mice. The data presented are means ± SE of three independent experiments (n = 4 for each genotype and each condition). *Statistically significant differences between wild-type and transgenic mice (*P < 0.001 and **P < 0.02 by one-factor ANOVA).

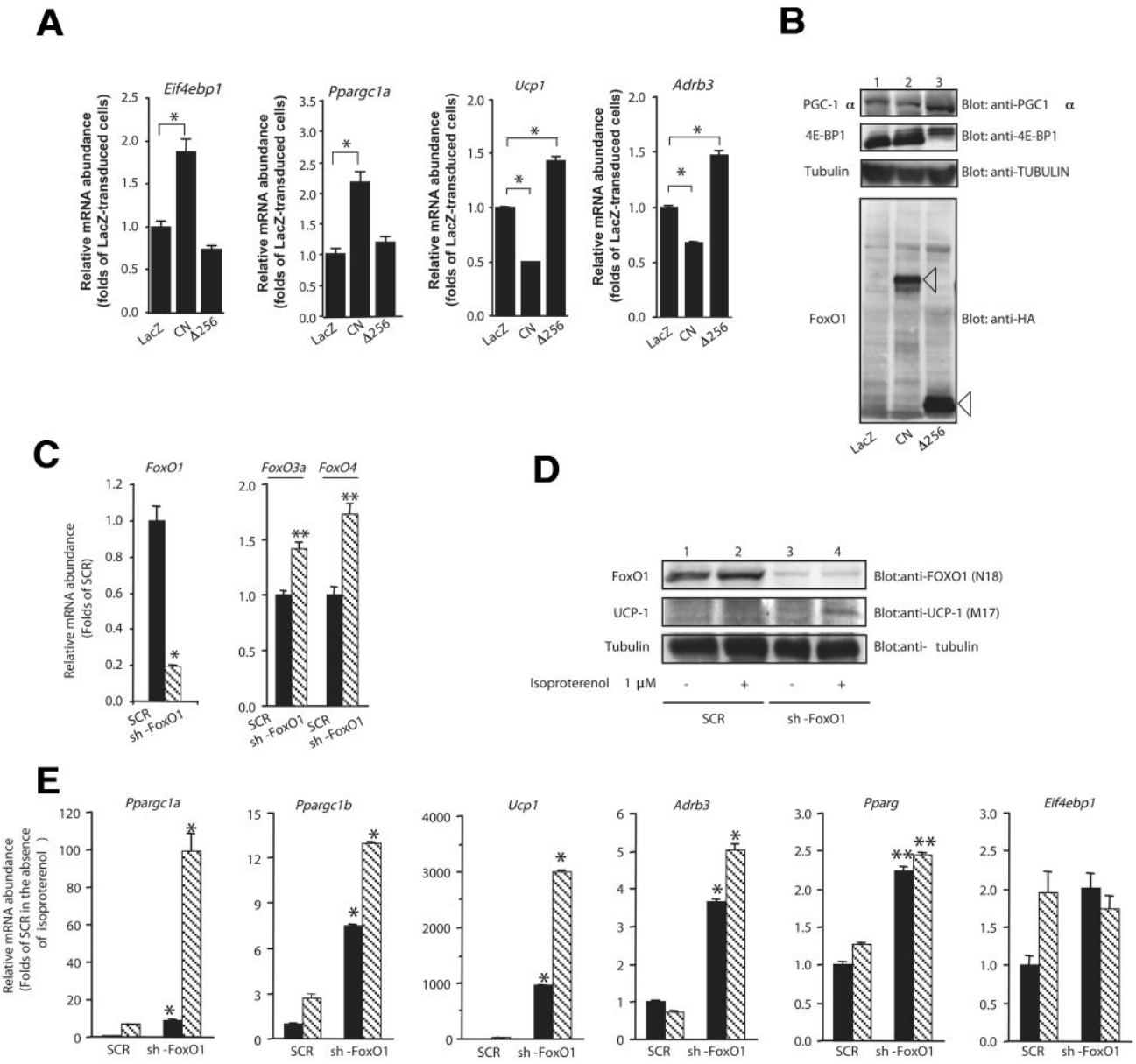

FIG. 6. Gene and protein expression in T37i cells infected with adenoviruses encoding the CN or Δ256 FoxO1 or transfected with shRNA of FoxO1. *A*: Real-time PCR of *Eif4ebp1*, *Ppargc1a*, *Ucp1*, and *Adrb3* using total RNA from T37i cells infected with adenoviruses encoding the indicated protein. The data presented are means ± SE of three independent experiments. *Statistically significant differences (P* < 0.05 by one-factor ANOVA). The CN indicates ADA FoxO1 in which threonine24, serine 253, and serine 316 are substituted to alanine or aspartic acid and the Δ256 indicates Δ256 FoxO1 (18). An arrow in *lane 2* or *3* in the *bottom panel* indicates the CN or Δ256 FoxO1, respectively. *B*: PGC-1α and 4E-BP1 protein expression in T37i cells infected with adenoviruses encoding indicated protein. *C*: Real-time PCR of *FoxOs* using total RNA from T37i cells transfected with shRNA of FoxO1 (sh-FoxO1) or a scrambled control shRNA (SCR). The data presented are means ± SE of three independent experiments. *Statistically significant differences (**P* < 0.005 and ***P* < 0.01 by one-factor ANOVA). *D*: Western blotting of lysates of T37i cells transfected with scrambled control shRNA (SCR) (*lanes 1* and *2*) or sh-FoxO1 (*lanes 3* and *4*) with the indicated antibodies. At day 5 after transfection and induction of differentiation, cells were incubated in the absence (*lanes 1* and *3*) or presence (*lane 2* and *4*) of 1 μmol/l isoproterenol for 6 h and harvested. *E*: Real-time PCR of *Ppargc1a*, *Ppargc1b*, *Ucp1*, *Ucp2*, *Adrb3*, *Pparg*, and *Eif4ebp1* using total RNA from T37i cells transfected with scrambled control shRNA (SCR) or sh-FoxO1 in the absence (■) or presence (▨) of 1 μmol/l of isoproterenol for 6 h. The data presented are means ± SE of three independent experiments. *Statistically significant differences between scrambled control shRNA and sh-FoxO1 in each condition (**P* < 0.001 and ***P* < 0.05 by one-factor ANOVA).**

significantly. Interestingly, although knockdown of FoxO1 increased *FoxO3a* and *FoxO4* expression, the molecular phenotype of T37i cells as brown adipocyte was enhanced. This finding suggests the hypothesis that FoxO1 may play a specific role in brown adipocyte among FoxOs. To elucidate the mechanism how FoxO1 affects differentiation of brown adipocytes, further investigations will be needed.

Several mechanisms of how FLAGΔ256 in adipose tissue improved glucose tolerance and insulin sensitivity can be speculated. We demonstrated that in WAT from transgenic mice, the ratio of small adipocytes was increased significantly compared with wild-type mice. Increased numbers of small adipocytes might contribute to improved glucose tolerance and insulin sensitivity despite increased visceral fat mass. The size of adipocytes is associated with insulin sensitivity (46). Failure in recruitment of new fat cells due to impaired differentiation may lead to a reduction in the capacity of adipose tissue to accumulate lipids and be paralleled by

enlargement of the existing adipocytes and also a "spill-over" and ectopic accumulation of lipids in other tissues, such as muscle and liver (47). Suppressed expression of several FoxO1 target genes, such as *Cdkn1b*, *Rb1*, *Rbl2*, and *Ccng2*, which are involved in cell cycle arrest, might increase proliferation of newly generated adipocytes. In addition, *Bcl2l11*, which induces cell death, expression level was also suppressed in WAT from transgenic mice. In addition, adipose tissue is an endocrine organ, which secretes several adipokines, such as adiponectin, leptin, and resistin. Enlargement of adipocytes might alter the amount of adipokines released (1). Expression of FLAGΔ256 in WAT affects gene expression, which includes increased expression of *Fasn*, *adiponectin*, *Slc2a4*, and *Pparg* and decreased expression of the *Tnf* and *Ccr2* genes. These changes of gene expression may improve insulin sensitivity under a high-fat diet. It has been already reported that FoxO1 repressed *Pparg* promoter activity and transcriptional regulation of *Slc2a4* (48). Therefore, the FLAGΔ256 may increase gene expression of *Pparg* and *Slc2a4*.

Transgenic mice in this study showed no significant difference of body weight a under high-fat diet, even though energy expenditure of transgenic mice was increased. This odd finding may be due to effects of FLAGΔ256 in WAT. In the present study, smaller adipocytes in WAT from transgenic mice were increased significantly compared with wild-type mice under a high-fat diet. These data suggest the possibility that overexpression of FLAGΔ256 might affect differentiation and proliferation of newly generated adipocytes. Furthermore, the finding that carbohydrate utilization of transgenic mice under a high-fat diet was increased suggests that triglyceride oxidation was spared and triglyceride accumulation was increased in WAT. Indeed, *Fasn* expression in WAT from transgenic mice was increased. Therefore, autonomous development of WAT may equalize increased energy expenditure and cause unchanged body weight.

The analyses using computed tomography revealed that visceral fat mass of transgenic mice is increased significantly compared with wild-type mice under a high-fat diet, although subcutaneous fat mass of *aP$_2$-FLAG-Δ256* mice is not changed. In general, increased mass of visceral adipose tissue has been known to produce a much greater risk of diabetes, dyslipidemia, and accelerated atherosclerosis than subcutaneous adipose tissue (49) (6). However, adipocytes of visceral fat from transgenic mice were small and could be considered to be insulin sensitive and overcome insulin resistance induced by a high-fat diet. The mechanism of how overexpression of FLAGΔ256 affects visceral and subcutaneous fat mass differentially is still unknown. However, it has been suggested that different adipocyte precursors are responsible for a specific adipose depot development and have a different pattern of gene expression of developmental genes (50). Therefore, these intrinsic differences between subcutaneous and visceral fats might affect differential phenotypes.

Conclusion. The present study demonstrated that the mutant FoxO1 increased energy store in WAT through increased small adipocytes and spared triglycerides and increased energy expenditure in BAT through enhanced thermogenic capacity of brown adipocytes. Therefore, it can be speculated that FoxO1 in adipose tissue might decrease energy store and energy expenditure. FoxO1 in adipose tissues may have an important role for changing energy homeostasis in response to excessive energy intake and identify FoxO1 as a potential target in treatment of obesity and its associated disorders, such as type 2 diabetes.

ACKNOWLEDGMENTS

This work was supported by a grant for the 21st Century Center of Excellence Program "Center of Excellence for Signal Transduction Disease: Diabetes Mellitus as a Model" from the Ministry of Education, Culture, Sports, Science and Technology of Japan; a grant from The Akiyama Foundation to J.N.; a grant from The Mother and Child Health Foundation to J.N.; a grant from Takeda Science Foundation to J.N.; and a grant from Uehara Memorial Foundation to J.N.

We thank Dr. Bruce M. Spiegelman (Dana-Farber Cancer Institute, Boston, MA) for kindly providing the promoter/enhancer fragment of the mouse *aP2* gene. We also thank Dr. Susumu Seino (Division of Cellular and Molecular Medicine, Kobe University Graduate School of Medicine) for making his laboratory available to accomplish this work kindly. We are also grateful to Dr. Mutsuo Taiji (Dainippon Sumitomo Pharmaceuticals) for kindly making a metabolic cage available. Y.O. is Research Fellow of the Japan Society for the Promotion of Science.

REFERENCES

1. Rosen ED, Spiegelman BM: Adipocytes as regulators of energy balance and glucose homeostasis. *Nature* 444:847–853, 2006
2. Barsh GS, Schwartz MW: Genetic approaches to studying energy balance: perception and integration. *Nat Rev Genet* 3:589–600, 2002
3. Lam TK, Schwartz GJ, Rossetti L: Hypothalamic sensing of fatty acids. *Nat Neurosci* 8:579–584, 2005
4. Kubota N, Yano W, Kubota T, Yamauchi T, Itoh S, Kumagai H, Kozono H, Takamoto I, Okamoto S, Shiuchi T, Suzuki R, Satoh H, Tsuchida A, Moroi M, Sugi K, Noda T, Ebinuma H, Ueta Y, Kondo T, Araki E, Ezaki O, Nagai R, Tobe K, Terauchi Y, Ueki K, Minokoshi Y, Kadowaki T: Adiponectin stimulates AMP-activated protein kinase in the hypothalamus and increases food intake. *Cell Metab* 6:55–68, 2007
5. Coll AP, Farooqi IS, O'Rahilly S: The hormonal control of food intake. *Cell* 129:251–262, 2007
6. Despres JP, Lemieux I: Abdominal obesity and metabolic syndrome. *Nature* 444:881–887, 2006
7. Okuno A, Tamemoto H, Tobe K, Ueki K, Mori Y, Iwamoto K, Umesono K, Akanuma Y, Fujiwara T, Horikoshi H, Yazaki Y, Kadowaki T: Troglitazone increases the number of small adipocytes without the change of white adipose tissue mass in obese Zucker rats. *J Clin Invest* 101:1354–1361, 1998
8. Cannon B, Houstek J, Nedergaard J: Brown adipose tissue: more than an effector of thermogenesis? *Ann N Y Acad Sci* 856:171–187, 1998
9. Puigserver P, Spiegelman BM: Peroxisome proliferator-activated receptor-gamma coactivator 1 alpha (PGC-1 alpha): transcriptional coactivator and metabolic regulator. *Endocr Rev* 24:78–90, 2003
10. Lowell BB, Spiegelman BM: Towards a molecular understanding of adaptive thermogenesis. *Nature* 404:652–660, 2000
11. Lin J, Wu PH, Tarr PT, Lindenberg KS, St-Pierre J, Zhang CY, Mootha VK, Jager S, Vianna CR, Reznick RM, Cui L, Manieri M, Donovan MX, Wu Z, Cooper MP, Fan MC, Rohas LM, Zavacki AM, Cinti S, Shulman GI, Lowell BB, Krainc D, Spiegelman BM: Defects in adaptive energy metabolism with CNS-linked hyperactivity in PGC-1alpha null mice. *Cell* 119:121–135, 2004
12. Guerra C, Navarro P, Valverde AM, Arribas M, Bruning J, Kozak LP, Kahn CR, Benito M: Brown adipose tissue-specific insulin receptor knockout shows diabetic phenotype without insulin resistance. *J Clin Invest* 108: 1205–1213, 2001
13. Tseng YH, Kriauciunas KM, Kokkotou E, Kahn CR: Differential roles of insulin receptor substrates in brown adipocyte differentiation. *Mol Cell Biol* 24:1918–1929, 2004
14. Valverde AM, Benito M, Lorenzo M: The brown adipose cell: a model for understanding the molecular mechanisms of insulin resistance. *Acta Physiol Scand* 183:59–73, 2005

15. Accili D, Arden KC: FoxOs at the crossroads of cellular metabolism, differentiation, and transformation. *Cell* 117:421–426, 2004
16. Onuma H, Vander Kooi BT, Boustead JN, Oeser JK, O'Brien RM: Correlation between FOXO1a (FKHR) and FOXO3a (FKHRL1) binding and the inhibition of basal glucose-6-phosphatase catalytic subunit gene transcription by insulin. *Mol Endocrinol* 20:2831–2847, 2006
17. Nakae J, Kitamura T, Kitamura Y, Biggs WH 3rd, Arden KC, Accili D: The forkhead transcription factor Foxo1 regulates adipocyte differentiation. *Dev Cell* 4:119–129, 2003
18. Nakae J, Kitamura T, Silver DL, Accili D: The forkhead transcription factor Foxo1 (Fkhr) confers insulin sensitivity onto glucose-6-phosphatase expression. *J Clin Invest* 108:1359–1367, 2001
19. Nakae J, Park BC, Accili D: Insulin stimulates phosphorylation of the forkhead transcription factor FKHR on serine 253 through a Wortmannin-sensitive pathway. *J Biol Chem* 274:15982–15985, 1999
20. Kanda H, Tamori Y, Shinoda H, Yoshikawa M, Sakaue M, Udagawa J, Otani H, Tashiro F, Miyazaki J, Kasuga M: Adipocytes from Munc18c-null mice show increased sensitivity to insulin-stimulated GLUT4 externalization. *J Clin Invest* 115:291–301, 2005
21. Nakae J, Biggs WH, Kitamura T, Cavenee WK, Wright CV, Arden KC, Accili D: Regulation of insulin action and pancreatic beta-cell function by mutated alleles of the gene encoding forkhead transcription factor Foxo1. *Nat Genet* 32:245–253, 2002
22. Nakae J, Cao Y, Daitoku H, Fukamizu A, Ogawa W, Yano Y, Hayashi Y: The LXXLL motif of murine forkhead transcription factor FoxO1 mediates Sirt1-dependent transcriptional activity. *J Clin Invest* 116:2473–2483, 2006
23. Imai T, Jiang M, Chambon P, Metzger D: Impaired adipogenesis and lipolysis in the mouse upon selective ablation of the retinoid X receptor alpha mediated by a tamoxifen-inducible chimeric Cre recombinase (Cre-ERT2) in adipocytes. *Proc Natl Acad Sci U S A* 98:224–228, 2001
24. Abel ED, Peroni O, Kim JK, Kim YB, Boss O, Hadro E, Minnemann T, Shulman GI, Kahn BB: Adipose-selective targeting of the GLUT4 gene impairs insulin action in muscle and liver. *Nature* 409:729–733, 2001
25. He W, Barak Y, Hevener A, Olson P, Liao D, Le J, Nelson M, Ong E, Olefsky JM, Evans RM: Adipose-specific peroxisome proliferator-activated receptor gamma knockout causes insulin resistance in fat and liver but not in muscle. *Proc Natl Acad Sci U S A* 100:15712–15717, 2003
26. Nakae J, Barr V, Accili D: Differential regulation of gene expression by insulin and IGF-1 receptors correlates with phosphorylation of a single amino acid residue in the forkhead transcription factor FKHR. *EMBO J* 19:989–996, 2000
27. Weisberg SP, Hunter D, Huber R, Lemieux J, Slaymaker S, Vaddi K, Charo I, Leibel RL, Ferrante AW Jr: CCR2 modulates inflammatory and metabolic effects of high-fat feeding. *J Clin Invest* 116:115–124, 2006
28. Greer EL, Brunet A: FOXO transcription factors at the interface between longevity and tumor suppression. *Oncogene* 24:7410–7425, 2005
29. Puig O, Marr MT, Ruhf ML, Tjian R: Control of cell number by Drosophila FOXO: downstream and feedback regulation of the insulin receptor pathway. *Genes Dev* 17:2006–2020, 2003
30. Junger MA, Rintelen F, Stocker H, Wasserman JD, Vegh M, Radimerski T, Greenberg ME, Hafen E: The Drosophila forkhead transcription factor FOXO mediates the reduction in cell number associated with reduced insulin signaling. *J Biol* 2:20, 2003
31. Southgate RJ, Neill B, Prelovsek O, El-Osta A, Kamei Y, Miura S, Ezaki O, McLoughlin TJ, Zhang W, Unterman TG, Febbraio MA: FOXO1 regulates the expression of 4E-BP1 and inhibits mTOR signaling in mammalian skeletal muscle. *J Biol Chem* 282:21176–21186, 2007
32. Tsukiyama-Kohara K, Poulin F, Kohara M, DeMaria CT, Cheng A, Wu Z, Gingras AC, Katsume A, Elchebly M, Spiegelman BM, Harper ME, Tremblay ML, Sonenberg N: Adipose tissue reduction in mice lacking the translational inhibitor 4E-BP1. *Nat Med* 7:1128–1132, 2001
33. Seale P, Kajimura S, Yang W, Chin S, Rohas LM, Uldry M, Tavernier G, Langin D, Spiegelman BM: Transcriptional control of brown fat determination by PRDM16. *Cell Metab* 6:38–54, 2007
34. Zennaro MC, Le Menuet D, Viengchareun S, Walker F, Ricquier D, Lombes M: Hibernoma development in transgenic mice identifies brown adipose tissue as a novel target of aldosterone action. *J Clin Invest* 101:1254–1260, 1998
35. Penfornis P, Viengchareun S, Le Menuet D, Cluzeaud F, Zennaro MC, Lombes M: The mineralocorticoid receptor mediates aldosterone-induced differentiation of T37i cells into brown adipocytes. *Am J Physiol Endocrinol Metab* 279:E386–E394, 2000
36. Cederberg A, Gronning LM, Ahren B, Tasken K, Carlsson P, Enerback S: FOXC2 is a winged helix gene that counteracts obesity, hypertriglyceridemia, and diet-induced insulin resistance. *Cell* 106:563–573, 2001
37. Wolfrum C, Shih DQ, Kuwajima S, Norris AW, Kahn CR, Stoffel M: Role of Foxa-2 in adipocyte metabolism and differentiation. *J Clin Invest* 112:345–356, 2003
38. Puigserver P, Rhee J, Donovan J, Walkey CJ, Yoon JC, Oriente F, Kitamura Y, Altomonte J, Dong H, Accili D, Spiegelman BM: Insulin-regulated hepatic gluconeogenesis through FOXO1-PGC-1alpha interaction. *Nature* 423:550–555, 2003
39. Park YS, Yoon Y, Ahn HS: Platycodon grandiflorum extract represses up-regulated adipocyte fatty acid binding protein triggered by a high fat feeding in obese rats. *World J Gastroenterol* 13:3493–3499, 2007
40. Medema RH, Kops GJ, Bos JL, Burgering BM: AFX-like forkhead transcription factors mediate cell-cycle regulation by Ras and PKB through p27kip1. *Nature* 404:782–787, 2000
41. Kops GJ, Medema RH, Glassford J, Essers MA, Dijkers PF, Coffer PJ, Lam EW, Burgering BM: Control of cell cycle exit and entry by protein kinase B-regulated forkhead transcription factors. *Mol Cell Biol* 22:2025–2036, 2002
42. Martinez-Gac L, Marques M, Garcia Z, Campanero MR, Carrera AC: Control of cyclin G2 mRNA expression by forkhead transcription factors: novel mechanism for cell cycle control by phosphoinositide 3-kinase and forkhead. *Mol Cell Biol* 24:2181–2189, 2004
43. Kops GJ, Dansen TB, Polderman PE, Saarloos I, Wirtz KW, Coffer PJ, Huang TT, Bos JL, Medema RH, Burgering BM: Forkhead transcription factor FOXO3a protects quiescent cells from oxidative stress. *Nature* 419:316–321, 2002
44. Dijkers PF, Medema RH, Lammers JW, Koenderman L, Coffer PJ: Expression of the pro-apoptotic Bcl-2 family member Bim is regulated by the forkhead transcription factor FKHR-L1. *Curr Biol* 10:1201–1204, 2000
45. Qiao L, Shao J: SIRT1 regulates adiponectin gene expression through Foxo1-C/enhancer-binding protein alpha transcriptional complex. *J Biol Chem* 281:39915–39924, 2006
46. Eriksson JW, Smith U, Waagstein F, Wysocki M, Jansson PA: Glucose turnover and adipose tissue lipolysis are insulin-resistant in healthy relatives of type 2 diabetes patients: is cellular insulin resistance a secondary phenomenon? *Diabetes* 48:1572–1578, 1999
47. Danforth E Jr: Failure of adipocyte differentiation causes type II diabetes mellitus? *Nat Genet* 26:13, 2000
48. Armoni M, Harel C, Karnieli E: Transcriptional regulation of the GLUT4 gene: from PPAR-gamma and FOXO1 to FFA and inflammation. *Trends Endocrinol Metab* 18:100–107, 2007
49. Rosen ED, MacDougald OA: Adipocyte differentiation from the inside out. *Nat Rev Mol Cell Biol* 7:885–896, 2006
50. Gesta S, Bluher M, Yamamoto Y, Norris AW, Berndt J, Kralisch S, Boucher J, Lewis C, Kahn CR: Evidence for a role of developmental genes in the origin of obesity and body fat distribution. *Proc Natl Acad Sci U S A* 103:6676–6681, 2006